ISSN 0915-633X

NATIONAL INSTITUTE FOR FUSION SCIENCE

The Non-axisymmetric Instability of the Wide-Gap Spherical Couette Flow

K. Araki, J. Mizushima and S. Yanase

(Received - Sep. 27, 1996)

NIFS-459 Oct. 1996

RESEARCH REPORT
NIFS Series

NAGOYA, JAPAN

The non-axisymmetric instability of the wide-gap spherical Couette flow.

Keisuke Araki*
Theory and Computer Simulation Center,
National Institute for Fusion Science, Nagoya 464-01, Japan

Jiro Mizushima
Department of Mechanical Engineering, Faculty of Engineering,
Doshisha University, Kyoto 610-03, Japan

Shinichiro Yanase
Engineering Mathematics, Faculty of Engineering,
Okayama University, Okayama 700, Japan

Abstract

The non-axisymmetric linear stability of the spherical Couette flow is investigated numerically when the ratio of gap width to inner sphere radius $(R_2 - R_1)/R_1 = 0.5$. The basic flow becomes unstable at $Re_c = 1245$ and the associated azimuthal wavenumber is $n_c = 5$, which agrees excellently with the experimental results by Egbers and Rath [*Acta Mech.* **81** (1990) pp.3-38]. The marginal mode is oscillatory and has the distinct wavy structure around the equator and the spiral structures extended in each hemisphere. Sufficiently large spatial resolution is found to be required in order to avoid a spuriously unstable eigenvalue that causes serious underestimation of the critical Reynolds number.

Keywords: spherical Couette flow, linear stability, supercritical Hopf bifurcation, spiral structure of the disturbance.

*e-mail address:kten@toki.theory.nifs.ac.jp

The spherical Couette flow has attracted many researchers not only from the industrial or the geophysical viewpoints but from the purely theoretical interest in its typical configuration. The system has variety of solutions though it has only two control parameters, the aspect ratio of the gap width to the inner sphere radius $\beta = (R_2 - R_1)/R_1$ where R_1, R_2 are the radii of inner and outer sphere respectively, and the Reynolds number $Re = \Omega R_1^2/\nu$ where Ω is angular velocity of the inner sphere and ν is the kinematic viscosity of the fluid. (The outer sphere is assumed to be fixed here.)

One of the interesting features which have been experimentally observed is that the transition from the basic laminar flow to the secondary one is qualitatively different according to the aspect ratio[1, 2]. When the gap is narrow ($\beta < 0.24$[2]), the first transition results in the formation of the secondary Taylor vortex around the equator and the axisymmetry of the flow is not broken. For wide gap cases ($\beta > 0.24$), on the contrary, the first transition is caused by a non-axisymmetric disturbance and a wavy spiral flow structure is formed.

Theoretical studies of the spherical Couette flow have been carried out mainly for the narrow gap cases and few have been done for the wide gap ones. Munson and Joseph studied the instability for the wide gap case in terms of the energy method and obtained the critical Reynolds number $Re_c = 90$ and the azimuthal wavenumber $n_c = 1$ of $\beta = 1$[3]. This result is, however, far from the experimentally observed value, $Re_c = 450$ and $n_c = 4$, for the same value of beta by Belyaev and Yavorskaya[4].

Our present scope is to bury this discrepancy between the experimental and the theoretical results of the instability problem for the wide gap case. In this report we restrict our attention to the case for $\beta = 0.5$. At this aspect ratio the transition to the spatially periodic non-axisymmetric flow is experimentally observed[1]. The critical Reynolds number is $Re_c = 1244$ and the azimuthal wavenumber is $n_c = 5$.

The basic flows that are axisymmetric and satisfy the incompressible stationary Navier-Stokes equations are obtained by the Newton-Raphson iterative method together with the collocation method. Velocity field $\mathbf{U}(\mathbf{r})$ is expressed in terms of the Stokes solution and the stream functions[5], which are expanded in the series of the modified Chebyshev polynomials $(1-x^2)\,T_m(x)$ and $(1-x^2)^2\,T_m(x)$ in r-direction and the derivative of Legendre polynomials $\sin\vartheta\,(\mathrm{d}/\mathrm{d}\vartheta)P_l(\cos\vartheta)$ in ϑ-direction.

The time dependence and φ-dependence of disturbance is assumed as $\mathbf{u}(\mathbf{r},t) = \mathbf{u}(r,\vartheta)\exp(\lambda t + in\varphi)$ where λ is a complex number and n is an assigned azimuthal wavenumber. The disturbance $\mathbf{u}(\mathbf{r})$ is expressed in terms of the toroidal and poloidal vector fields[6]. The stream functions are expanded in the series of the modified Chebyshev polynomials given above and the Legendre bipolynomials $P_l^n(\cos\vartheta)$. The double QR method together with the collocation method is adopted to solve the eigenvalue problem.

In the present study we examined the cases with the Reynolds numbers Re =1100, 1200, 1300, 1400 and 1500 and with the wavenumbers $1 \le n \le 8$. The neutral Reynolds number for each n is determined by interpolation of the obtained growth rates data. The critical Reynolds number Re_c and the associated wavenumber n_c are given by the lowest of these neutral values and its wavenumber.

It should be remarked that the basic flow is symmetric with respect to the equator so that the linear stability analysis can be carried out separately according to the symmetry of the eigenmodes with respect to the equator. Hence we carried out the calculations using only the expansion functions with assigned symmetry in

ϑ-direction. In the following we use the notation (M,N) to denote the truncation number in r- and ϑ-directions respectively where N is the number of expansion functions with assigned symmetry. It is found that the basic flow is stable against all the equatorially symmetric disturbances when $Re = 1500$. Thus we report the results of the equatorially antisymmetric disturbances in the following.

Convergence of eigenvalue is checked by increasing (M,N) of the eigenvalue problem while (M,N) of basic flow is fixed to (17,129). The values of the numerically obtained growth rates $\mathrm{Re}(\lambda)$ for assigned (M,N) are listed in Table.1. It is verified that the convergence of the growth rates is guaranteed upto two digits when (M,N) is larger than (17,65). The smaller the truncation number becomes, the larger the growth rate becomes remarkably, therefore, the more seriously the critical Reynolds number is underestimated. In this study calculations are carried out with the truncation numbers (17,129) for the basic flows and (17,65) for linear stability analysis. The eigenvalue problem with (17,65) truncation modes requires about 340 MB memories and it costs about 1000 seconds CPU time in NEC SX-3 supercomputer for a set of parameters, Re and n.

The most unstable eigenvalues have complex values for all the calculated parameters. The values of growth rates for each Re and n are plotted in Fig.1. The numerically obtained critical Reynolds number is $Re_c = 1245$ which is surprisingly close to the experimentally observed value $Re_c = 1244$. The associated wavenumber is $n_c = 5$ which also coincides with the observed value.

In Fig.2 the phase velocity normalized by the angular velocity of the inner boundary, $\omega = \mathrm{Im}(\lambda)/(n\Omega)$, are plotted. It is remarkable that the normalized phase velocities almost depend on neither the Reynolds number nor the wave numbers when $n \geq 3$. In Fig.3 the values of $n\omega$, which represents the frequency of a spiral arms observed at a fixed point, are plotted by white circles for $n = 5$. Solid circles in the same figure are the experimentally observed values for $n = 5$[1]. The agreement of the experimental data and the numerical results is very good. These numerical results are also consistent with the following experimental observation: the frequency of spiral arms changes after the transition to the state with different number of spiral arms and the frequency is proportional to the numbers of spiral arms.

The numerical results obtained here explain the experimental data quite well though present analysis is the linear stability theory. This suggests that the observed spiral flow is well approximated by the sum of the basic axisymmetric flow and the weak unstable disturbance. Therefore the bifurcation is expected to be the supercritical Hopf one.

It is interesting that the basic flow $\mathbf{U}(\mathbf{r})$ has two distinct flow structures (see Fig.4(a)). One is the strong radial shear near the inner boundary. The other is the strong meridional shear localized in the equatorial region. We will call these structures as the *inner boundary layer* and the *equatorial jet* respectively. The region outside these two structures is tentatively called as the *outer layer.*

The thickness of the inner boundary layer is about 20 % of the gap width and it does not depend on the latitude when the thickness is defined in terms of the amplitude of the angular velocity $U_\varphi/(r \sin \vartheta)$.

The equatorial jet is formed around the equator. Because the meridional "stagnation" flow conveys outward the angular momentum which the fluid in the inner boundary layer carries (see Fig.4(b)).

The outer layer has relatively uniform angular velocity. The amplitude of the angular velocity in this region is about 20 % of that of the inner sphere. It is interesting that this value is close to the phase velocity of the unstable disturbance.

In Fig.4(c) a section of the azimuthal component of the unstable disturbance is depicted. The unstable disturbance has a distinct wavy structure which is almost confined in the equatorial jet region. Another distinct structure is found in the outer layer. As is seen in Fig.5 this is a spiral structure which corresponds with the experimentally observed one. There is a structure inside the inner boundary layer and its amplitude is relatively small. Thus these structures of the unstable disturbance can be divided into three parts which almost correspond to those of the basic flow.

These flow structures seem to be generated as follows. The equatorial jet becomes unstable and a Tollmien-Schlichting wave is excited on it as the Reynolds number increases. This localized wave vibrates the fluids in the outer layer so that the excited motion obliquely propagates at an angle 58° from the equator like a Rossby wave. Thus the spiral arms which are experimentally observed is generated. We are now working on the quantitative analysis of both the basic flow and the unstable disturbance.

Acknowledgment

The authors thank Prof. Nagata for introducing us the Ref.1.

References

[1] C. Egbers and H. J. Rath, The existence of Taylor vortices and wide-gap instabilities in spherical Couette flow, Acta Mech. **111** (1995) pp.125-140.

[2] Yu. N. Belyaev, A. A. Monakhov and I. M. Yavorskaya, Stability of spherical Couette flow in thick layers when the inner sphere revolves, Fluid Dyn. **13** (1978) pp.162-168. [Transl. Izv. Akad. Nauk SSSR. Mekhanika Zhidkosti i Gaza, No. 2, pp.9-15, March-April, 1978]

[3] B. R. Munson and D. D. Joseph, Viscous incompressible flow between concentric rotating spheres. Part 2. Hydrodynamic stability, J. Fluid Mech. **49** (1971) pp.305-318.

[4] Yu. N. Belyaev and I. M. Yavorskaya, Transition to stochasticity of viscous flow between rotating spheres, in *Nonlinear Dynamics and Turbulence* edited by G. I. Barenblatt, G. Iooss, and D. D. Joseph (Pitman, Boston, 1983) pp.61-70.

[5] B. R. Munson and D. D. Joseph, Viscous incompressible flow between concentric rotating spheres. Part 1. Basic flow, J. Fluid Mech. **49** (1971) pp.289-303.

[6] S. Chandrasekhar, *Hydrodynamic and hydromagnetic stability*, (Clarendon, Oxford, 1961) Appendix III.

(M , N)	n = 1	n = 5
(9 , 33)	460.182	178.601
(10 , 39)	386.006	120.853
(11 , 41)	300.541	64.7601
(12 , 45)	204.294	3.48202
(13 , 49)	111.839	2.65884
(14 , 53)	17.3107	2.51514
(15 , 57)	−9.30994	2.77549
(16 , 61)	−11.4163	2.79538
(17 , 65)	−12.0544	7.76952
(18 , 69)	−12.3066	7.73299
(19 , 73)	−12.4292	7.76631

Table.1. Convergence of the growth rate as the truncation number of the disturbance increases. Parameters are $Re = 1500$ and $n = 1$, 5. Truncation number of the basic flow is (17,129).

Figure Captions

Fig.1. Growth rates of disturbance Re(λ) for assigned n's. Symbols denote azimuthal wavenumber; × :1, ○ :2, △ :3, □ :4, ● :5, ▲ :6, ■ :7, + :8. The thick line is obtained by linear least square fitting for the data of n=5. The double circle is the critical Reynolds number obtained by the experiment [1].

Fig.2. Normalized phase velocities for assigned n's. The same symbols as Fig.1 are used to assign the wavenumbers.

Fig.3. Ratio of the frequency of spiral arms observed at a fixed point to that of inner sphere rotation $n\omega$=(Im(λ)/Ω) for n = 5; ○: numerical results, ●: experimental data from Ref.[1].

Fig.4. Meridional sections of the flow when $Re = 1500$ and $n = 5$: (a) U_φ and (b) the meridional stream function of the basic flow, (c) a meridional section of u_φ of the unstable disturbance. Increment is 10 % of each peak value.

Fig.5. Horizontal section of u_r of the unstable disturbance at $r = (R_1 + 3R_2)/4$. Increment is 20 % of the peak value.

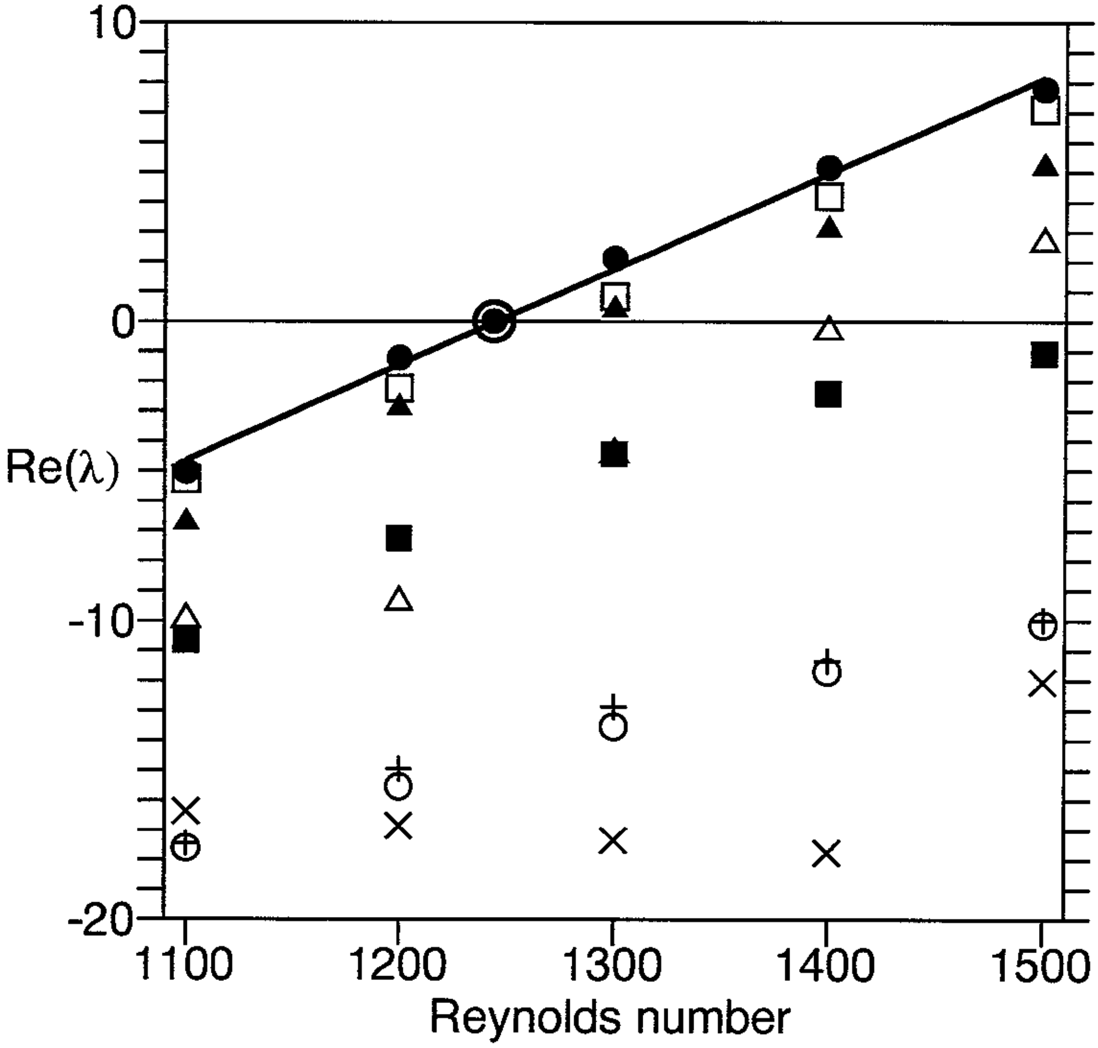

Fig.1

K. Araki, J. Mizushima and S. Yanase

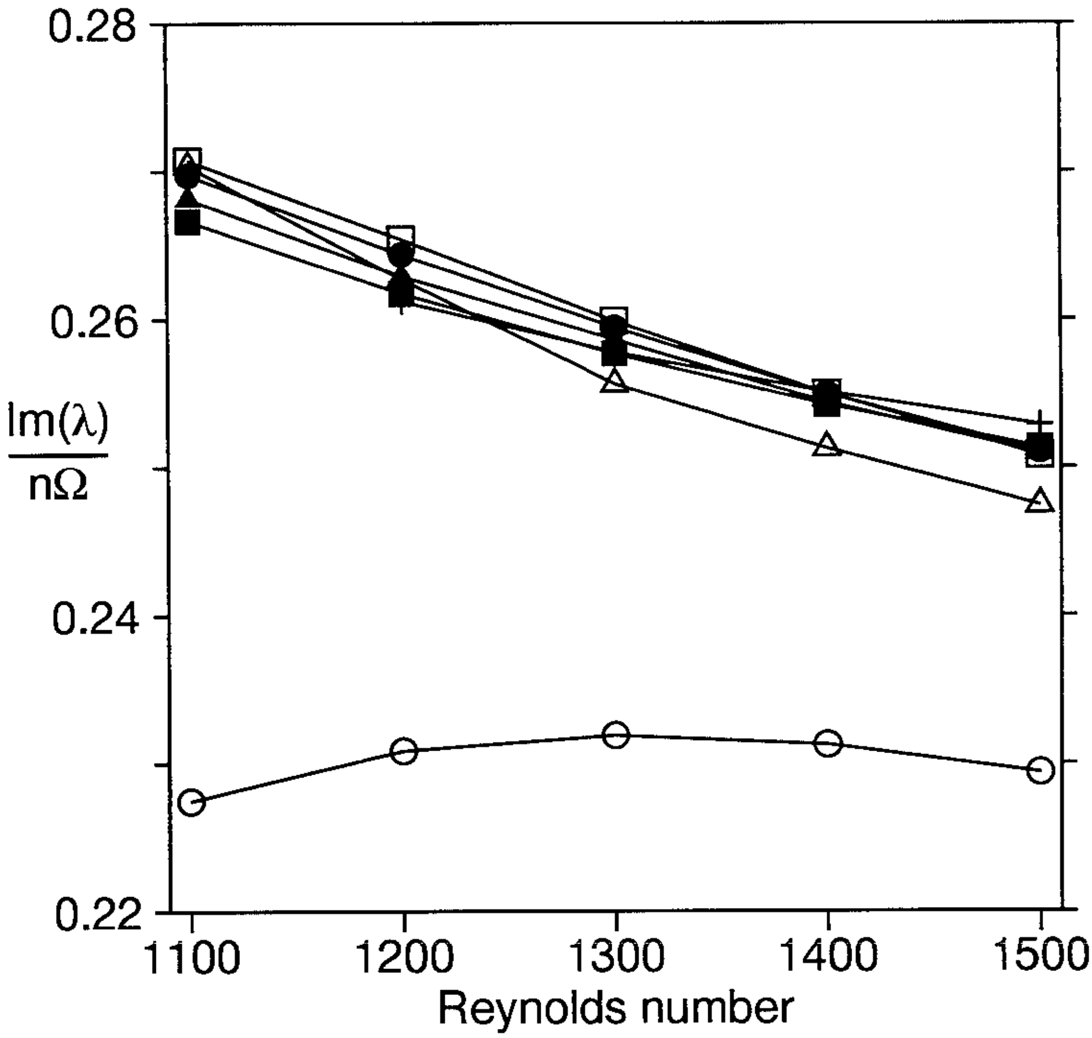

Fig.2

K. Araki, J. Mizushima and S. Yanase

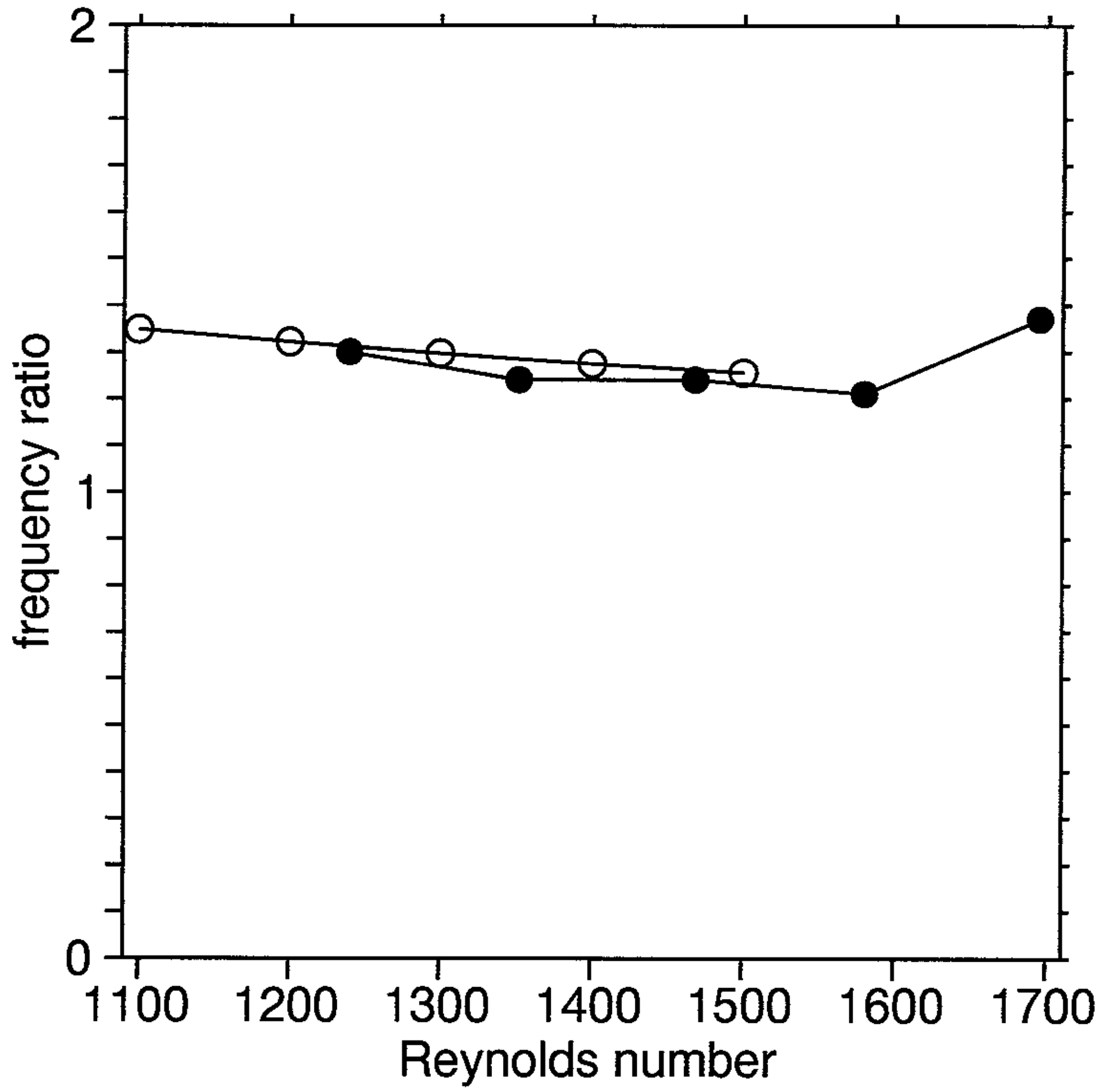

Fig.3

K. Araki, J. Mizushima and S. Yanase

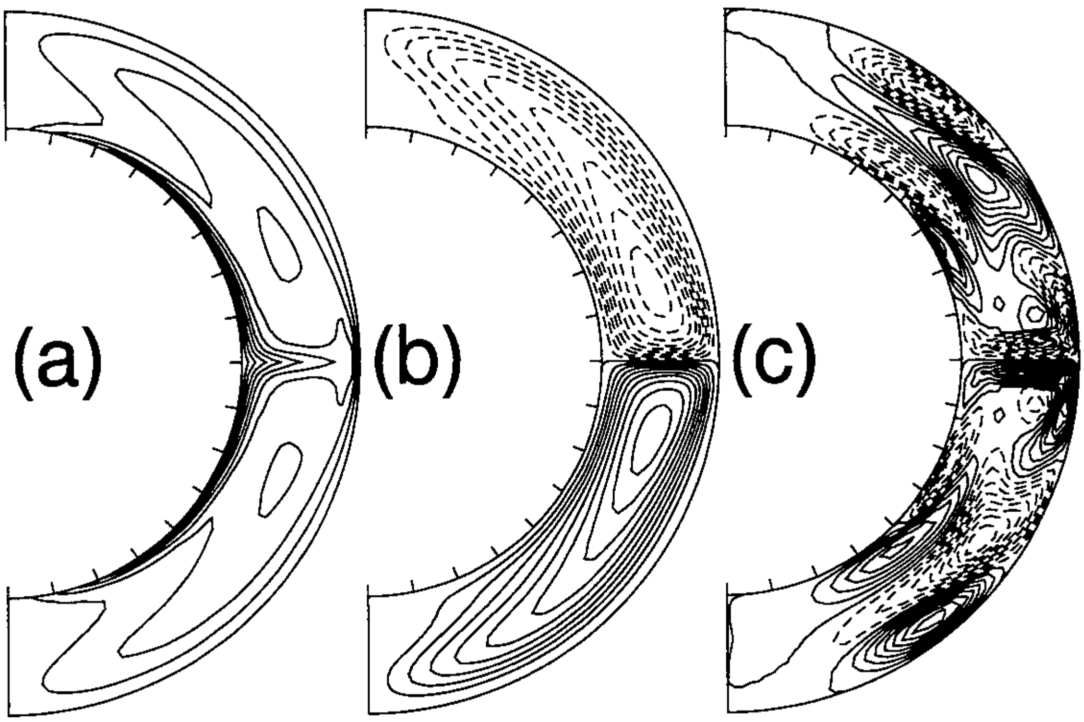

Fig.4

K. Araki, J. Mizushima and S. Yanase

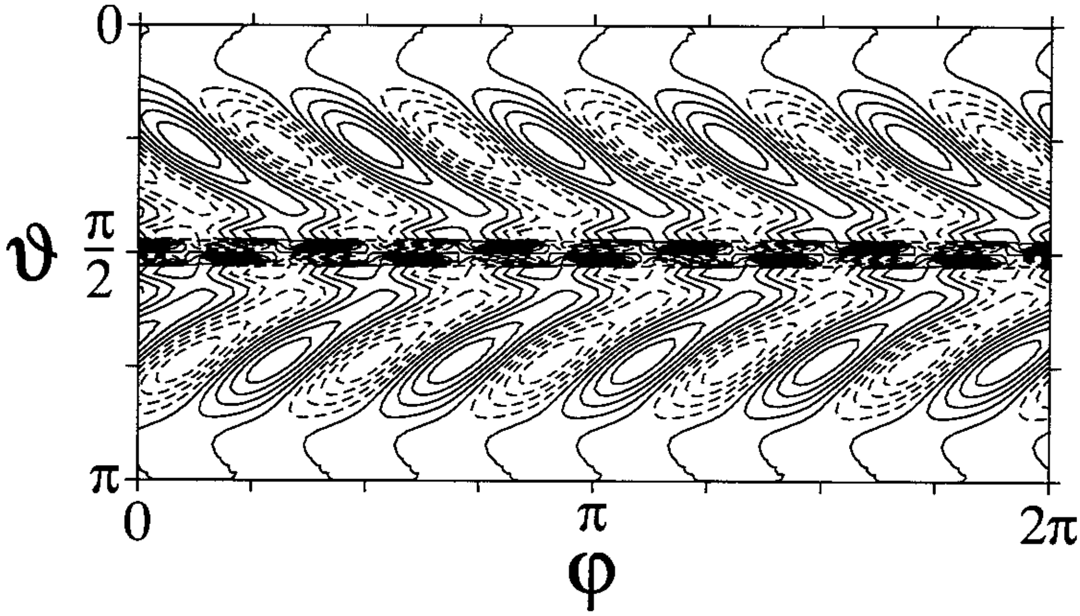

Fig.5

K. Araki, J. Mizushima and S. Yanase

Recent Issues of NIFS Series

NIFS-422 Y. Kondoh, M. Yamaguchi and K. Yokozuka,
Simulations of Toroidal Current Drive without External Magnetic Helicity Injection; July 1996

NIFS-423 Joong-San Koog,
Development of an Imaging VUV Monochromator in Normal Incidence Region. July 1996

NIFS-424 K. Orito,
A New Technique Based on the Transformation of Variables for Nonlinear Drift and Rossby Vortices; July 1996

NIFS-425 A. Fujisawa, H. Iguchi, S. Lee, T.P. Crowley, Y. Hamada, H. Sanuki, K. Itoh, S. Kubo, H. Idei, T. Minami, K. Tanaka, K. Ida, S. Nishimura, S. Hidekuma, M. Kojima, C. Takahashi, S. Okamura and K. Matsuoka,
Direct Observation of Potential Profiles with a 200keV Heavy Ion Beam Probe and Evaluation of Loss Cone Structure in Toroidal Helical Plasmas on the Compact Helical System; July 1996

NIFS-426 H. Kitauchi, K. Araki and S. Kida,
Flow Structure of Thermal Convection in a Rotating Spherical Shell; July 1996

NIFS-427 S. Kida and S. Goto,
Lagrangian Direct-interaction Approximation for Homogeneous Isotropic Turbulence; July 1996

NIFS-428 V.Yu. Sergeev, K.V. Khlopenkov, B.V. Kuteev, S. Sudo, K. Kondo, F. Sano, H. Zushi, H. Okada, S. Besshou, T. Mizuuchi, K. Nagasaki, Y. Kurimoto and T. Obiki,
Recent Experiments on Li Pellet Injection into Heliotron E; Aug. 1996

NIFS-429 N. Noda, V. Philipps and R. Neu,
A Review of Recent Experiments on W and High Z Materials as Plasma-Facing Components in Magnetic Fusion Devices; Aug. 1996

NIFS-430 R.L. Tobler, A. Nishimura and J. Yamamoto,
Design-Relevant Mechanical Properties of 316-Type Stainless Steels for Superconducting Magnets; Aug. 1996

NIFS-431 K. Tsuzuki, M. Natsir, N. Inoue, A. Sagara, N. Noda, O. Motojima, T. Mochizuki, T. Hino and T. Yamashina,
Hydrogen Absorption Behavior into Boron Films by Glow Discharges in Hydrogen and Helium; Aug. 1996

NIFS-432 T.-H. Watanabe, T. Sato and T. Hayashi, *Magnetohydrodynamic Simulation on Co- and Counter-helicity Merging of Spheromaks and Driven Magnetic Reconnection*; Aug. 1996

NIFS-433 R. Horiuchi and T. Sato,
Particle Simulation Study of Collisionless Driven Reconnection in a Sheared Magnetic Field; Aug. 1996

NIFS-434 Y. Suzuki, K. Kusano and K. Nishikawa,
Three-Dimensional Simulation Study of the Magnetohydrodynamic Relaxation Process in the Solar Corona. II.; Aug. 1996

NIFS-435 H. Sugama and W. Horton,
Transport Processes and Entropy Production in Toroidally Rotating Plasmas with Electrostatic Turbulence; Aug. 1996

NIFS-436 T. Kato, E. Rachlew-Källne, P. Hörling and K.-D Zastrow,
Observations and Modelling of Line Intensity Ratios of OV Multiplet Lines for 2s3s 3S1 - 2s3p 3Pj; Aug. 1996

NIFS-437 T. Morisaki, A. Komori, R. Akiyama, H. Idei, H. Iguchi, N. Inoue, Y. Kawai, S. Kubo, S. Masuzaki, K. Matsuoka, T. Minami, S. Morita, N. Noda, N. Ohyabu, S. Okamura, M. Osakabe, H. Suzuki, K. Tanaka, C. Takahashi. H. Yamada, I. Yamada and O. Motojima,
Experimental Study of Edge Plasma Structure in Various Discharges on Compact Helical System; Aug. 1996

NIFS-438 A. Komori, N. Ohyabu, S. Masuzaki, T. Morisaki, H. Suzuki, C. Takahashi, S. Sakakibara, K. Watanabe, T. Watanabe, T. Minami, S. Morita, K. Tanaka, S. Ohdachi, S. Kubo, N. Inoue, H. Yamada, K. Nishimura, S. Okamura, K. Matsuoka, O. Motojima, M. Fujiwara, A. Iiyoshi, C. C. Klepper, J.F. Lyon, A.C. England, D.E. Greenwood, D.K. Lee, D.R. Overbey, J.A. Rome, D.E. Schechter and C.T. Wilson,
Edge Plasma Control by a Local Island Divertor in the Compact Helical System; Sep. 1996 (IAEA-CN-64/C1-2)

NIFS-439 K. Ida, K. Kondo, K. Nagaski T. Hamada, H. Zushi, S. Hidekuma, F. Sano, T. Mizuuchi, H. Okada, S. Besshou, H. Funaba, Y. Kurimoto, K. Watanabe and T. Obiki,
Dynamics of Ion Temperature in Heliotron-E; Sep. 1996 (IAEA-CN-64/CP-5)

NIFS-440 S. Morita, H. Idei, H. Iguchi, S. Kubo, K. Matsuoka, T. Minami, S. Okamura, T. Ozaki, K. Tanaka, K. Toi, R. Akiyama, A. Ejiri, A. Fujisawa, M. Fujiwara, M. Goto, K. Ida, N. Inoue, A. Komori, R. Kumazawa, S. Masuzaki, T. Morisaki, S. Muto, K. Narihara, K. Nishimura, I. Nomura, S. Ohdachi, M.. Osakabe, A. Sagara, Y. Shirai, H. Suzuki, C. Takahashi, K. Tsumori, T. Watari, H. Yamada and I. Yamada,
A Study on Density Profile and Density Limit of NBI Plasmas in CHS; Sep. 1996 (IAEA-CN-64/CP-3)

NIFS-441 O. Kaneko, Y. Takeiri, K. Tsumori, Y. Oka, M. Osakabe, R. Akiyama, T. Kawamoto, E. Asano and T. Kuroda,
Development of Negative-Ion-Based Neutral Beam Injector for the Large Helical Device; Sep. 1996 (IAEA-CN-64/GP-9)

NIFS-442 K. Toi, K.N. Sato, Y. Hamada, S. Ohdachi, H. Sakakita, A. Nishizawa, A. Ejiri, K. Narihara, H. Kuramoto, Y. Kawasumi, S. Kubo, T. Seki, K. Kitachi, J. Xu, K. Ida, K. Kawahata, I. Nomura, K. Adachi, R. Akiyama, A. Fujisawa, J. Fujita, N. Hiraki, S. Hidekuma, S. Hirokura, H. Idei, T. Ido, H. Iguchi, K. Iwasaki, M. Isobe, O. Kaneko, Y. Kano, M. Kojima, J. Koog, R. Kumazawa, T. Kuroda, J. Li, R. Liang, T. Minami, S. Morita, K. Ohkubo, Y. Oka, S. Okajima, M. Osakabe, Y. Sakawa, M. Sasao, K. Sato, T. Shimpo, T. Shoji, H. Sugai, T. Watari, I. Yamada and K. Yamauti,
Studies of Perturbative Plasma Transport, Ice Pellet Ablation and Sawtooth Phenomena in the JIPP T-IIU Tokamak; Sep. 1996 (IAEA-CN-64/A6-5)

NIFS-443 Y. Todo, T. Sato and The Complexity Simulation Group,
Vlasov-MHD and Particle-MHD Simulations of the Toroidal Alfvén Eigenmode; Sep. 1996 (IAEA-CN-64/D2-3)

NIFS-444 A. Fujisawa, S. Kubo, H. Iguchi, H. Idei, T. Minami, H. Sanuki, K. Itoh, S. Okamura, K. Matsuoka, K. Tanaka, S. Lee, M. Kojima, T.P. Crowley, Y. Hamada, M. Iwase, H. Nagasaki, H. Suzuki, N. Inoue, R. Akiyama, M. Osakabe, S. Morita, C. Takahashi, S. Muto, A. Ejiri, K. Ida, S. Nishimura, K. Narihara, I. Yamada, K. Toi, S. Ohdachi, T. Ozaki, A. Komori, K. Nishimura, S. Hidekuma, K. Ohkubo, D.A. Rasmussen, J.B. Wilgen, M. Murakami, T. Watari and M. Fujiwara,
An Experimental Study of Plasma Confinement and Heating Efficiency through the Potential Profile Measurements with a Heavy Ion Beam Probe in the Compact Helical System; Sep. 1996 (IAEA-CN-64/C1-5)

NIFS-445 O. Motojima, N. Yanagi, S. Imagawa, K. Takahata, S. Yamada, A. Iwamoto, H. Chikaraishi, S. Kitagawa, R. Maekawa, S. Masuzaki, T. Mito, T. Morisaki, A. Nishimura, S. Sakakibara, S. Satoh, T. Satow, H. Tamura, S. Tanahashi, K. Watanabe, S. Yamaguchi, J. Yamamoto, M.Fujiwara and A. Iiyoshi,
Superconducting Magnet Design and Construction of LHD; Sep. 1996 (IAEA-CN-64/G2-4)

NIFS-446 S. Murakami, N. Nakajima, S. Okamura, M. Okamoto and U. Gasparino,
Orbit Effects of Energetic Particles on the Reachable β–Value and the Radial Electric Field in NBI and ECR Heated Heliotron Plasmas; Sep. 1996 (IAEA-CN-64/CP -6) Sep. 1996

NIFS-447 K. Yamazaki, A. Sagara, O. Motojima, M. Fujiwara, T. Amano, H. Chikaraishi, S. Imagawa, T. Muroga, N. Noda, N. Ohyabu, T. Satow, J.F. Wang, K.Y. Watanabe, J. Yamamoto . H. Yamanishi, A. Kohyama, H. Matsui, O. Mitarai, T. Noda, A.A. Shishkin, S. Tanaka and T. Terai
Design Assessment of Heliotron Reactor; Sep. 1996 (IAEA-CN-64/G1-5)

NIFS-448 M. Ozaki, T. Sato and the Complexity Simulation Group,
Interactions of Convecting Magnetic Loops and Arcades; Sep. 1996

NIFS-449 T. Aoki,
Interpolated Differential Operator (IDO) Scheme for Solving Partial Differential Equations; Sep. 1996

NIFS-450 D. Biskamp and T. Sato,
Partial Reconnection in the Sawtooth Collapse; Sep. 1996

NIFS-451 J. Li, X. Gong, L. Luo, F.X. Yin, N. Noda, B. Wan, W. Xu, X. Gao, F. Yin, J.G. Jiang, Z. Wu., J.Y. Zhao, M. Wu, S. Liu and Y. Han,
Effects of High Z Probe on Plasma Behavior in HT-6M Tokamak; Sep. 1996

NIFS-452 N. Nakajima, K. Ichiguchi, M. Okamoto and R.L. Dewar,
Ballooning Modes in Heliotrons/Torsatrons; Sep. 1996 (IAEA-CN-64/D3-6)

NIFS-453 A. Iiyoshi,
Overview of Helical Systems; Sep. 1996 (IAEA-CN-64/O1-7)

NIFS-454 S. Saito, Y. Nomura, K. Hirose and Y.H. Ichikawa,
Separatrix Reconnection and Periodic Orbit Annihilation in the Harper Map; Oct. 1996

NIFS-455 K. Ichiguchi, N. Nakajima and M. Okamoto,
Topics on MHD Equilibrium and Stability in Heliotron / Torsatron; Oct. 1996

NIFS-456 G. Kawahara, S. Kida, M. Tanaka and S. Yanase,
Wrap, Tilt and Stretch of Vorticity Lines around a Strong Straight Vortex Tube in a Simple Shear Flow; Oct. 1996

NIFS-457 K. Itoh, S.- I. Itoh, A. Fukuyama and M. Yagi,
Turbulent Transport and Structural Transition in Confined Plasmas; Oct. 1996

NIFS-458 A. Kageyama and T. Sato,
Generation Mechanism of a Dipole Field by a Magnetohydrodynamic Dynamo; Oct. 1996

NIFS-459 K. Araki, J. Mizushima and S. Yanase,
The Non-axisymmetric Instability of the Wide-Gap Spherical Couette Flow; Oct. 1996